Available online at www.sciencedirect.com
SCIENCE DIRECT®
Journal of Power Sources 119–121 (2003) 205–210
JOURNAL OF POWER SOURCES
www.elsevier.com/locate/jpowsour

Lithium intercalation in electrodeposited vanadium oxide bronzes

E. Andrukaitis*

Air Vehicles Research Section, Defence R&D Canada Atlantic, 101 Colonel By Drive, Ottawa, Ont., Canada K1A 0K2

Abstract

By using an electrodeposition method to form hexavanadates, followed by a thermal process, a range of bronze stoichiometries, $M_xV_6O_{13+y}$, where M: K, Ni, or Mo, $0 < x < 0.5$, $0.2 < y < 3.3$ in the ternary system of V_2O_4–V_2O_5–M_2O were prepared. These bronzes adhered well to a conducting substrate and could be directly fabricated into a coin cell without the need for binders or electronic conductors. The phase changes on discharge and the lithium insertion ability were influenced by the amount of the guest metal in the bronze structure. When the value of x was small (<0.5) reversible phase changes resembled those of V_2O_5 or V_6O_{13} depending on the initial O_2 content of the bronze after heating. The cycle life was adversely affected by the depth of discharge below 2.2 V for the V_2O_5 type bronzes. The V_6O_{13} bronze cathodes had better cycle lives at average operating voltages of about 2.5 V and over 350 Ah/kg for their initial cycles.

Keywords: Lithium insertion; Lithium intercalation; Vanadium oxide; Transition metal oxides; Vanadium oxide bronzes

1. Introduction

The pure vanadium oxides that have made the largest advances for use as rechargeable lithium battery systems, are V_2O_5, LiV_3O_8 and V_6O_{13} [1]. Other bronze phases, such as $M_xV_2O_5$, where M: Li, Na, K, Cs, Mg, Ca or Ag, were also examined as insertion electrodes [2–5] and reversible intercalation depended on the guest cation species. Recent work on transition metal vanadate cathodes prepared using low-temperature synthesis techniques has shown high specific capacities [6,7]. As well, the V_2O_5 xerogel and aerogel-like morphologies have yielded specific capacities above 500 Ah/kg [8,9] at low discharge rates. In this study, crystalline vanadium oxide bronzes were made by electrodepositing vanadates on a conducting substrate and heating to form the bronzes, $M_xV_6O_{13+y}$, where M: K, Ni, or Mo, $0 < x < 0.5$, $0.2 < y < 3.3$, in the ternary system of V_2O_4–V_2O_5–M_2O, where M: K, Ni, or Mo. Because the bronze adheres well to the substrate, no binders or electronic conducting materials were added to the bronze cathode in a lithium coin cell. Fabricating the bronze cathodes in this manner was a useful tool in studying Li intercalation properties into pure crystalline materials without any interference from traditional electrode additives. This could allow for more reliable electrochemical performance measures of these bronzes, avoid use of flooded electrolyte cells which impede long-term cycling experiments and generally reduce the risk of mechanical failure of the electrode assembly.

2. Experimental

Materials were cleaned and prepared as described previously [10]. Solutions for electrodeposition of NH_4VO_3 solution were prepared at 50 °C. Electrodeposits were doped with other transition metals by adding small concentrations of either potassium or nickel chloride or ammonium molybdate. Electrodeposits were formed on conducting substrates of 150 stainless steel mesh by cyclic voltammetry from +0.2 to −0.7 V (SCE) at 50 mV/s for several hours. The deposits were then decomposed at temperatures from 300 to 400 °C under air or argon atmospheres. The materials were analysed by atomic absorption (AA), powder X-ray diffraction (XRD), scanning electron microscopy (SEM) and differential scanning calorimetry (DSC) methods. The mass of the electrode (electrodeposit and substrate) was also measured before assembly and after cycling the electrode in a coin cell. The active material (bronze) on the electrode was then dissolved in mild sulphuric acid solution in an ultrasonic bath and then analysed by AA. The mass of the substrate was weighed again after removal of the active material.

Amorphous vanadium pentoxide gels were prepared using an ion-exchange resin and aged for several months. They were air dried and mixed with 20 wt.% Ketjen black and then cast on the same 150 stainless steel mesh substrate. The gels were dried under vacuum to up to 200 °C and their mass

* Tel.: +1-613-990-0638; fax: +1-613-993-4095.
E-mail address: ed.andrukaitis@nrc.ca (E. Andrukaitis).

0378-7753/03/$ – see front matter.
doi:10.1016/S0378-7753(03)00180-0

was measured. Cathodes of the bronzes were prepared in a coin cell using an electrolyte composed of 1 M $LiPF_6$ dissolved in 1:1 of ethylene carbonate and dimethyl carbonate (EC:DMC) and a counter electrode of Li metal. The cells were then discharged and charged galvanostatically at a current density of 0.1–1 mA/cm^2 (Arbin 2024 Cycler).

3. Results

3.1. Physical characteristics of the bronzes

Using the electrodeposition method, tetra-ammonium hexavanadates ($(NH_4)_4V_6O_{16}$), can be deposited on a conducting substrate. By addition of an alkali metal or transition metal salt to the deposition solution it is possible to form metal-ammonium hexavanadates with the stoichiometry, $(NH_4)_xM_{4-x}V_6O_{16}$. The alkali metal hexavanadates of K, Rb and Cs made in this way have been characterised in a previous paper [11]. When these electrodeposits are subjected to a thermal process, a range of bronzes can be formed in the ternary system of V_2O_4–V_2O_5–M_2O (Fig. 1a). The decomposition/bronze formation process has been discussed for the alkali metal hexavanadates of K, Rb and Cs [12]. When heated in air, an oxidation of the hexavanadate occurs by the overall reaction:

$$(NH_4)_xM_{4-x}V_6O_{16} + \tfrac{1}{2}yO_2 \rightarrow M_{4-x}V_6O_{16+y-(x/2)} + xNH_3 + \tfrac{1}{2}xH_2O \quad (1)$$

When heated in an argon atmosphere (no oxygen present), reduction occurs by the overall reaction:

$$(NH_4)_xM_{4-x}V_6O_{16} \rightarrow M_{4-x}V_6O_{16-y-(x/2)} + xNH_3 + \tfrac{1}{2}xH_2O + \tfrac{1}{2}yO_2 \quad (2)$$

By X-ray diffraction and chemical analysis, for values of $3.5 < x < 4.0$, when heated in air, a crystalline V_2O_5

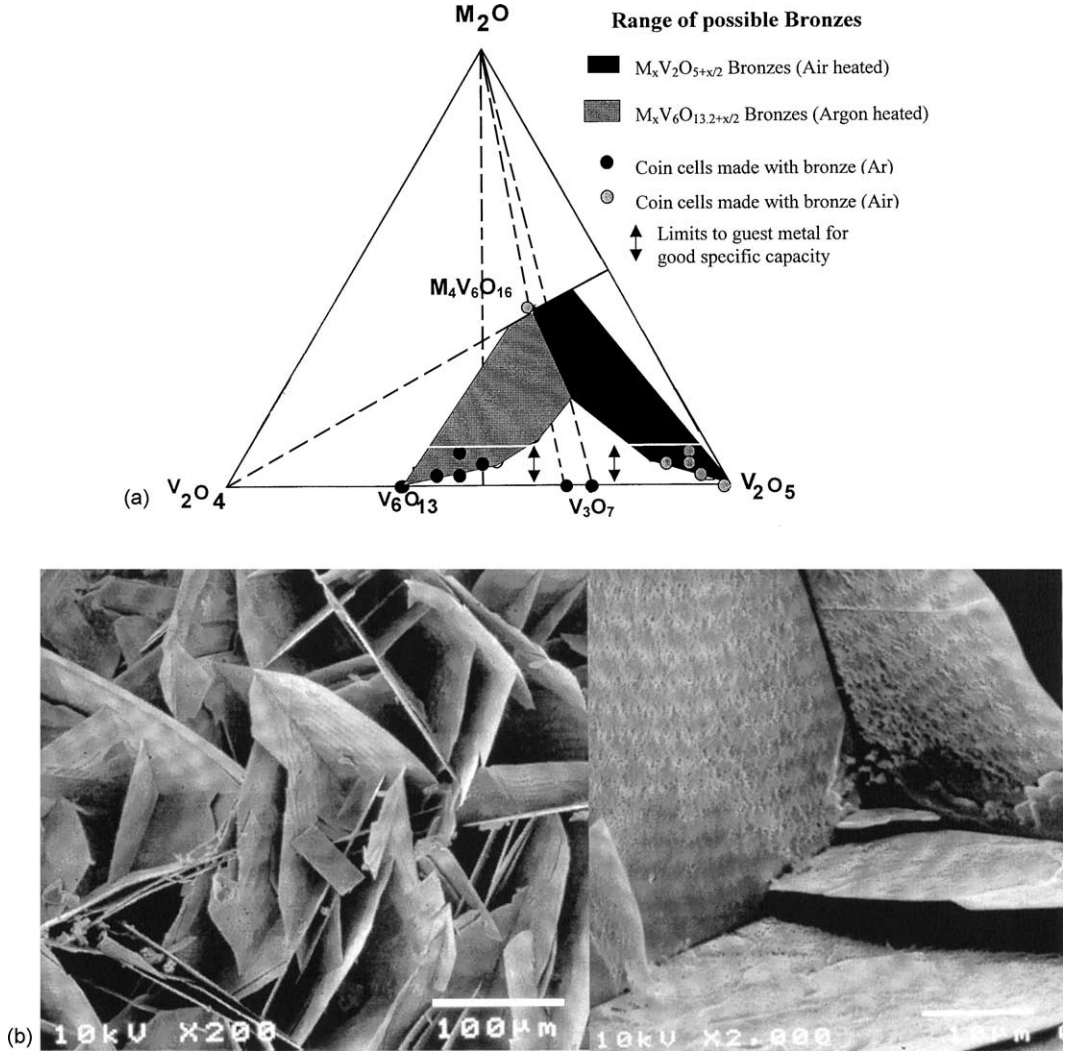

Fig. 1. (a) Phase diagram showing the range of bronze stoichiometries that can be synthesised in the ternary system, V_2O_4–V_2O_5–M_2O, where M: K, Ni, or Mo, for heated electrodeposits in air (dark area) or argon (shaded area). (b) Scanning electron microscopy photograph of a vanadium oxide bronze electrodeposit after heating to 350 °C on a stainless steel mesh electrode. (A) Magnification at 200× and (B) magnification at 2000×.

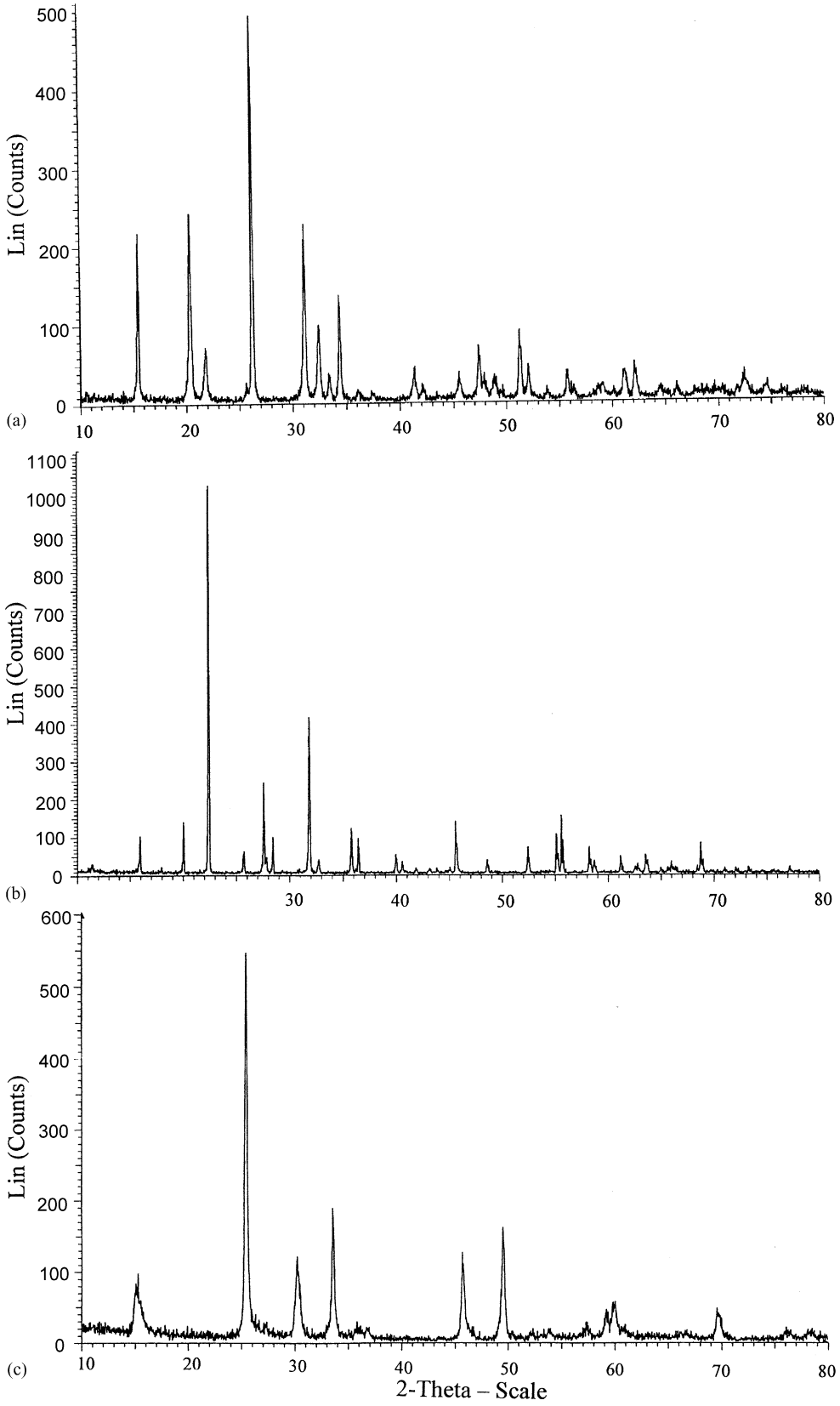

Fig. 2. X-ray diffraction patterns of unheated and thermally decomposed electrodeposits: (a) air heated (V_2O_5) at 350 °C for 10 h, (b) unheated electrodeposit ($(NH_4)_4V_6O_{16}$) and (c) heated under argon stream ($V_6O_{13.2}$) for 10 h at 350 °C.

Table 1
Lattice parameters for the X-ray diffraction patterns of unheated and thermally decomposed electrodeposits with comparison to literature values

(A) Unheated tetra-ammonium hexavanadate $(NH_4)_4V_6O_{16}$ tetragonal *P4bm*
$a = 8.917$, $c = 5.587$ [15]
$a = 8.932$, $c = 5.593$, this paper
(B) Air heated electrodeposit V_2O_5 orthorhombic *Pmmn*
$a = 11.519$, $b = 3.564$, $c = 4.373$, volume = 179.53 [16]
$a = 11.49$, $b = 3.567$, $c = 4.370$, volume = 179.1, this paper
(C) Heated under argon atmosphere V_6O_{13} monoclinic *C2/m*
$a = 11.922$, $b = 3.680$, $c = 10.138$, beta = 100.87, volume = 436.8 [17]
$a = 11.95$, $b = 3.69$, $c = 9.96$, beta = 103, volume = 439, this paper

(A) Unheated electrodeposit, (B) air heated at 350 °C for 10 h, and (C) heated under argon stream for 10 h at 350 °C.

structure is formed when oxygen is added in the approximate range of $1.0 < y < 2.0$ (Eq. (1)).

However, when heated under argon, a disordered, non-stoichiometric V_6O_{13} structure is formed when oxygen is removed in the approximate range $0.4 < y < 0.9$ (Eq. (2)). The complete thermal oxidation of V(IV) to V(V) in the ammonium hexavanadate occurs more readily than partial reduction of V(V) to V(IV) to form stoichiometric V_6O_{13}.

The X-ray diffraction patterns for an unheated electrodeposit and the air or argon heated electrodeposits are shown in Fig. 2. The unit cell dimensions agree very well with those reported in the literature as shown in Table 1 [13–15]. However, as was confirmed using chemical analysis, the XRD pattern of the electrodeposit thermally decomposed under Ar forms a disordered structure with a non-stoichiometric range of about $V_6O_{13.1}$ to about $V_6O_{13.3}$. These results were similar to those found for the decomposition of NH_4VO_3 to form $V_6O_{13.19}$ by Abraham et al. [16]. Further reduction to form a more stoichiometric V_6O_{13} bronze is currently being investigated by changing the heating regime. Also, any increase in guest transition metal over $x < 3.8$ gave increasingly disordered structures by XRD. This was linked to the incomplete oxidation/reduction of vanadium during the heating process [12].

The bronzes made in this study adhered very well to a conducting substrate and were directly fabricated into a coin cell without the need for binders or electronic conductors. As shown in the SEM photographs, the electrodeposited bronzes were highly oriented and layered structures, giving a high bulk surface area, which should allow for good contact to occur with the liquid electrolyte (Fig. 1b). Structural changes taking place during heating of the electrodeposits to form vanadium oxide bronzes had no effect on the strong adherence of these materials to the substrate. This means a very strong bonding action occurs during electrodeposition, which is needed to study electrochemical properties. For example, use of a ''sticky-carbon'' electrode was used to characterise vanadium oxide aerogels because agglomeration occurs when composite electrodes are formed in the usual manner [17,18].

3.2. Electrochemical study of bronzes

Although the cathodes from the SEM photographs had an irregular, rough surface and no electronic conductors were used, complete utilisation of the active material was possible in an actual coin cell construction. This was confirmed by mass and AA analysis of the cathode material on the substrate before and after cycling. The electrodeposition/thermal decomposition process to form vanadium bronzes on a conducting substrate yielded cathode materials with good mechanical properties for electrochemical studies.

Results for V_2O_5 bronze electrodeposits had similar results to previous work where cycling above 2.5 V gave excellent cycle life (Table 2) (Fig. 1a) [1,19]. A trade-off between energy density and cycle life exists for the V_2O_5 bronzes, with the irreversible formation of new structures when they are discharged below 2.5 V [20,21]. Although initial capacities of over 250 Ah/kg were achievable if discharged below 2.0 V, the benefit on continuous deep cycling of anything below 2.2 V was quickly lost after about 15–20 cycles. The amorphous V_2O_5 gels prepared with 20 wt.% carbon displayed good initial cycle life, with an initial specific capacity of about 225 mAh/g (600 Wh/kg) at *C*/40 to 2.0 V (Table 2). It has been reported that twice the specific energy is possible (1250 Wh/kg) ($n = 4$) using V_2O_5 XRG, but at a very low discharge rate of *C*/100–200 [9]. A recent paper using a more practical *C*/5 rate for a V_2O_5 aerogel reported that the degree of Li intercalation initially was $n = 2.53$ and decreased to $n = 1.8$ (71%) by the 16th cycle [22] in $Li_nV_2O_5$. The problem with the V_2O_5 gels was the difficulty of fabricating enough material on a

Table 2
Specific capacity and specific energy of various electrodeposited vanadium oxide bronzes in a lithium coin cell at 0.1 mA/cm^2

Material	Voltage range (V)	Initial specific capacity (Ah/kg)	Specific energy (Wh/kg)	Specific capacity of initial (%)
V_2O_5	3.7–2.7	145	475	90 (500)
	3.7–2.0	236	680	70 (15)
$V_6O_{13.2}$	3.7–2.0	320	814	80 (100)
	3.7–1.5	375	911	75 (10)
$K_{0.2}V_6O_{15.1}$	3.7–2.0	295	805	>80 (15)
	3.7–1.8	378	968	60 (15)
$Ni_{1.0}V_6O_{15.9}$	3.7–2.0	189	470	78 (55)
	3.7–1.8	351	800	70 (40)
$Mo_{0.2}V_6O_{15.7}$	3.7–2.0	300	685	77 (35)
	3.7–1.5	355	775	80 (25)
$Mo_{0.2}V_6O_{13.8}$	3.7–2.0	300	685	77 (35)
	3.7–1.5	355	775	80 (25)
V_2O_5 gel	3.8–2.0	225	596	96 (16)
	3.8–1.5	260	665	99 (10)
V_2O_5 aerogel [23]	3.8–1.4	350	875	71 (16)

Values shown in parentheses are cycle number.

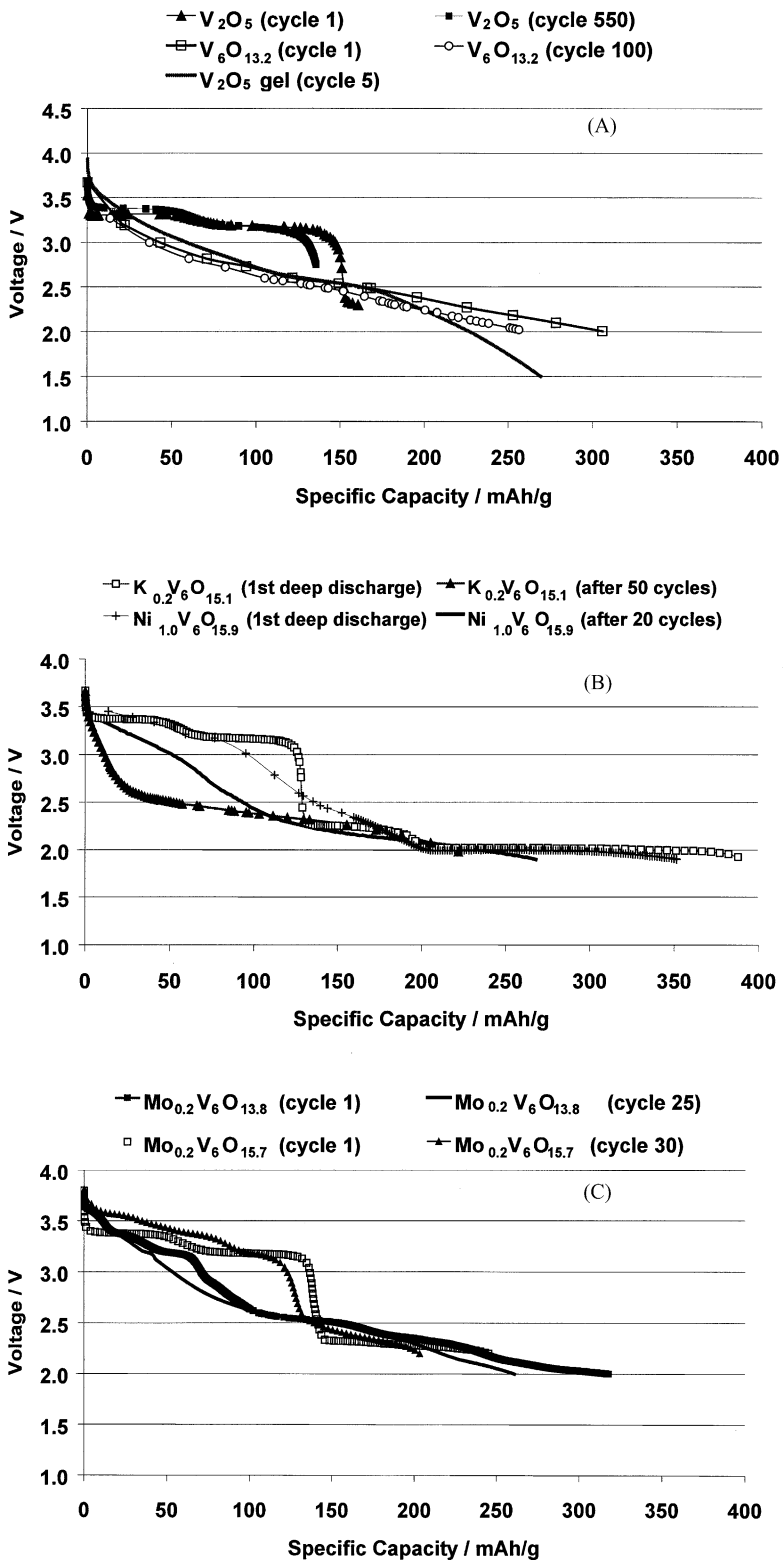

Fig. 3. Plot of the voltage vs. the specific capacity for the initial discharge and after cycling of electrodeposited cathodes in a coin cell with a lithium metal anode and 1 M $LiPF_6$ in 1:1 EC:DMC electrolyte at 0.2 mA/cm^2: (A) V_2O_5, $V_6O_{13\cdot2}$ and V_2O_5, gel cathodes, (B) $K_{0\cdot2}V_6O_{15\cdot1}$ and $Ni_{1.0}V_6O_{15.9}$ cathodes and (C) $Mo_{0.2}V_6O_{13.8}$ and $Mo_{0.2}V_6O_{15.7}$ cathodes.

conducting substrate and in sufficient quantity (thickness) to provide significant capacity for use in a cell or battery, and residual water is present even after drying up to 200 °C.

The non-stoichiometric V_6O_{13} bronzes have a better overall cycling behaviour for deep discharge regimes compared to the V_2O_5 bronzes (Table 1). They could also be discharged to lower voltages (1.5 V) with lower fade rates than the V_2O_5 bronzes or gels, with an initial capacity of 375 Ah/kg achieved. This was close to the predicted very high theoretical capacity of 420 Ah/kg predicted for V_6O_{13} ($n = 8$, where n is the number of transferred electrons per molecular unit) [23]. However, the capacity fell to about 75% of the initial value after 10 deep cycles to 1.5 V. Best cycling results were similar to previous work when cycling was carried out to a maximum of $n = 6$, or to about 2.0 V [1]. Initial capacities of 320 Ah/kg and over 100 cycles with <80% loss of capacity were achieved with pure bronze cathode electrodes. Failure of the coin cells appears related to problems at the lithium anode as was previously observed by others for composite electrodes or thin films [1].

When introducing a guest metal species in the vanadium oxide bronze structure, the phase changes on discharge and the lithium insertion ability were influenced by the amount included. When the value of guest metal species was small, reversible phase changes resembled those of V_2O_5 or V_6O_{13}, depending on the O_2 content of the $M_{4-x}V_6O_{16-y-(x/2)}$ bronze discussed above (Fig. 3B and C). The presence of too much of another guest metal in the bronze structure decreases the specific capacity of the bronze. This is largely because V_2O_5 has a layered structure with the guest metal lying between the layers [14]. Thus, too much of a guest metal interferes with the lithium intercalation/removal process. However, results have shown that some benefit comes from small amounts of metal "impurities" in the bronze structure. Improvement in the capacity fade and specific capacity when deep discharging some V_2O_5 bronzes was observed (Table 2). This could be due to similar reasons why non-stoichiometric $V_6O_{13.19}$ can accommodate more lithium than stoichiometric V_6O_{13} [19].

4. Conclusions

Formation of vanadium oxide bronzes by an electrodeposition/thermal process to form rechargeable cathode materials directly onto a conducting substrate has been demonstrated. Because the vanadium oxide cathodes adhere well to the substrate, no binders or electronic conductors were needed to achieve good rechargeable performance comparable to composite vanadium oxides studied in the past. Vanadium bronzes that had a structure of non-stoichiometric V_6O_{13} gave the best cycling versus specific capacity performance compared to V_2O_5 bronzes or gels. The amount of a guest metal in the vanadium bronze influenced the performance and rate capability. Some benefit in cycle life and specific capacity was found for the V_2O_5 bronzes if a guest metal was included in small quantities.

Acknowledgements

The author wishes to thank Giulio Torlone of the National Research Council, Institute for Chemical Process and Environmental Technology and staff at ICPET for technical assistance.

References

[1] J. Desilvestro, O. Haas, J. Electrochem. Soc. 137 (1990) 5C–22C.
[2] I. Raistrick, R. Huggins, Mater. Res. Bull. 18 (1983) 337.
[3] I. Raistrick, Rev. Chim. Miner. 21 (1984) 456.
[4] J.P. Pereira-Ramos, R. Messina, J. Perichon, J. Electrochem. Soc. 135 (1988) 3050–3057.
[5] V. Manev, A. Momchilov, A. Nassalevska, G. Pistoia, M. Pasquali, J. Power Sources 43–44 (1993) 561.
[6] S. Denis, E. Baudrin, F. Orsini, G. Ouvrard, M. Touboul, J.M. Tarascon, J. Power Sources 81–82 (1999) 79–84.
[7] E. Andrukaitis, G.L. Torlone, I.R. Hill, J. Power Sources 81–82 (1999) 651–655.
[8] P.P. Prosini, S. Passerini, R. Vellone, W.H. Smyrl, J. Power Sources 75 (1998) 73–83.
[9] B.B. Owens, W.H. Smyrl, J.J. Xu, J. Power Sources 81–82 (1999) 150–155.
[10] E. Andrukaitis, P.W.M. Jacobs, J.W. Lorimer, Solid State Ionics 37 (1990) 157.
[11] E. Andrukaitis, P.W. Jacobs, J.W. Lorimer, Can. J. Chem. 68 (1990) 1283–1292.
[12] E. Andrukaitis, J. Power Sources 54 (1995) 470–474.
[13] J. Bernard, F. Theobald, A. Vidonne, Bull. Soc. Chim. Fr. 6 (1970) 2108.
[14] H.G. Bachman, F.R. Ahmed, W.H. Barnes, Z. Kristallog. Kristallgeom. Kristallphys. Kristallchem. 115 (1961) 110.
[15] K. Wilhelmi, K. Walterson, L. Kihlborg, Acta Chem. Scand. 25 (1971) 2675.
[16] K.M. Abraham, J.L. Goldman, M.D. Dempsey, J. Electrochem. Soc. 128 (1981) 2493.
[17] W. Dong, D.R. Rolison, B. Dunn, Eletrochem. Solid-State Lett. 3 (2000) 457–459.
[18] W. Long, D.R. Rolison, New directions in electroanalytical chemistry II, in: J. Leddy, P. Vanysek, M.D. Porter (Eds.), The Electrochemical Society Proceedings Series, Pennington, NJ, 1999, p. 121.
[19] K.M. Abraham, J. Power Sources 7 (1981–1982) 1.
[20] K. West, B. Zachau-Christiansen, T. Jacobsen, J. Power Sources 43–44 (1993) 127–134.
[21] C. Delmas, S. Bethes, M. Menetrier, J. Power Sources 34 (1991) 113–118.
[22] A.N. Mansour, P.H. Smith, in: Proceedings of the 7th Workshop for Battery Development, Philadelphia, PA, USA, 5–28 June 2001, pp. 83–87.
[23] K. West, B. Zachau-Christiansen, T. Jacobsen, Electrochim. Acta 28 (1983) 1829.